Free Radical Research, March 2006; 40(3): 303–320

Taylor & Francis
Taylor & Francis Group

Interactions of quercetin with iron and copper ions: Complexation and autoxidation

HAKIMA EL HAJJI[1], EZZOHRA NKHILI[2], VALERIE TOMAO[3], & OLIVIER DANGLES[3]

[1]*Faculté des Sciences et Techniques-Guéliz, Université Cadi Ayyad, Marrakech, Morocco,* [2]*Faculté des Sciences Semlalia, Université Cadi Ayyad, Marrakech, Morocco, and* [3]*UMR A 408 INRA—Université d'Avignon, 33, rue Louis Pasteur, Avignon 84029, France*

Accepted by Professor B. Halliwell

(Received 18 October 2005; in revised form 2 November 2005)

Free Radic Res Downloaded from informahealthcare.com by Library of Health Sci-Univ of Il on 11/30/11
For personal use only.

Abstract

Quercetin (3,3′,4′,5,7-pentahydroxyflavone), one of the most abundant dietary flavonoids, has been investigated for its ability to bind Fe^{II}, Fe^{III}, Cu^{I} and Cu^{II} in acidic to neutral solutions. In particular, analysis by UV–visible spectroscopy allows to determine the rate constants for the formation of the 1:1 complexes. In absence of added metal ion, quercetin undergoes a slow autoxidation in neutral solution with production of low hydrogen peroxide (H_2O_2) concentrations. Autoxidation is accelerated by addition of the metal ions according to: $Cu^{I} > Cu^{II} \gg Fe^{II} \approx Fe^{III}$. In fact, the iron-quercetin complexes seem less prone to autoxidation than free quercetin in agreement with the observation that EDTA addition, while totally preventing iron-quercetin binding, slightly accelerates quercetin autoxidation. By contrast, the copper-quercetin complexes appear as reactive intermediates in the copper-initiated autoxidation of quercetin. In presence of the iron ions, only low concentrations of H_2O_2 can be detected. By contrast, in the presence of the copper ions, H_2O_2 is rapidly accumulated. Whereas Fe^{II} is rapidly autoxidized to Fe^{III} in the presence or absence of quercetin, Cu^{I} bound to quercetin or its oxidation products does not undergo significant autoxidation. In addition, Cu^{II} is rapidly reduced by quercetin. By HPLC-MS analysis, the main autoxidation products of quercetin are shown to be the solvent adducts on the *p*-quinonemethide intermediate formed upon two-electron oxidation of quercetin. Finally, in strongly acidic conditions (pH 1–2), neither autoxidation nor metal complexation is observed but Fe^{III} appears to be reactive enough to quickly oxidize quercetin (without dioxygen consumption). Up to *ca.* 7 Fe^{III} ions can be reduced per quercetin molecule, which points to an extensive oxidative degradation.

Keywords: *Quercetin, flavonoid, metal, iron, copper, complexation*

Introduction

Flavonoids (the main class of polyphenols) are abundant in all parts of plants and in plant-derived foods such as common fruits and vegetables, tea and wine. Beside their important functions in plants, (pigmentation, UV screening, iron uptake, chemical defense against predators, participation in signalling pathways leading to N_2 fixation etc.) they have attracted considerable interest over the last two decades because of their important role in defining the organoleptic properties of foods (colour, flavour) and, possibly, their nutritional value in terms of preventing the development of degenerative diseases (cardiovascular diseases, cancers, age-related disorders) [1–5]. This last point is substantiated by a wealth of *in vitro* studies that point to the ability of flavonoids to act as antioxidants, enzyme inhibitors and modulators of various biochemical signals.

Interactions of flavonoids with metal ions is also a biologically significant process. For instance, iron complexation has been proposed as a possible antioxidant mechanism in plant nodules where the highly reducing conditions allowing N_2 reduction

Correspondence: O. Dangles, UMR A 408 INRA—Université d'Avignon, 33, rue Louis Pasteur, Avignon 84029, France. Tel: 33 490 14 44 46. Fax: 33 490 14 44 41. E-mail: olivier.dangles@univ-avignon.fr

ISSN 1071-5762 print/ISSN 1029-2470 online © 2006 Taylor & Francis
DOI: 10.1080/10715760500484351

RIGHTSLINK

Free Radic Res Downloaded from informahealthcare.com by Library of Health Sci-Univ of Il on 11/30/11
For personal use only.

could also lead to O_2 activation with subsequent production of reactive oxygen species (ROS) and oxidative damage to biomolecules [6]. Moreover, complexation of dietary iron in the gastro-intestinal tract is known to lower iron bioavailability and may favour disorders related to iron deficiency, especially in developing countries (anti-nutritional effect) [7]. More generally, the reducing properties of flavonoids and their ability to form stable complexes with iron and copper ions can strongly modulate the redox properties of those metal ions and sustain part of the antioxidant and, eventually, pro-oxidant properties of flavonoids [6,8–16]. This pro-oxidant/antioxidant balance is highly dependent on the environment, especially the presence of other metal chelators and the targeted biomolecules. For instance, flavonoids stimulate Fe^{III}-induced hydroxyl radical production from H_2O_2 in the presence of EDTA but not in the presence of citrate or ATP [8]. In the absence of chelators, production of the hydroxyl radical by the Fenton reaction ($Fe^{II} + H_2O_2$) was also promoted by highly reducing flavonoids such as quercetin [10]. Usually, when lipid peroxidation is initiated by iron- or copper-containing systems, the antioxidant activity of flavonoids prevails [6,9–13] and likely operates by a combination of radical scavenging and metal complexation processes. On the other hand, pro-oxidant and antioxidant effects of flavonoids have been reported in the metal-induced oxidative degradation of proteins and DNA (in the absence or presence of hydroperoxides) [6,14–16]. The pro-oxidant activity of flavonoids can be related to their ability to reduce high-valence metal ions (Fe^{III}, Cu^{II}) into their low-valence counterparts (Fe^{II}, Cu^{I}), which can either autoxidize or promote the homolytic cleavage of hydroperoxides with subsequent ROS production. Finally, highly reducing flavonoids are air-sensitive compounds that may undergo autoxidation to yield ROS [17,18]. This poorly understood process is likely mediated by metal traces [19,20] and may participate in flavonoid cytotoxicity, not only because of the ROS produced but also because some flavonoid oxidation products (e.g. aryloxyl radicals, *o*-quinones and *p*-quinonemethides) are highly oxidant and/or electrophilic [21–26]. Finally, flavonoid autoxidation is probably a major cause of flavonoid instability during the processing of flavonoid-containing foods, especially during thermal treatments [27].

In this work, interactions of quercetin (3,3′,4′,5,7-pentahydroxyflavone), one of the most abundant flavonoid aglycones, with iron and copper ions are investigated in acidic to neutral aqueous solutions. The rate constants and thermodynamic constants of metal complexation are estimated. The influence of added metal ions on the kinetics of quercetin autoxidation and H_2O_2 production is also studied as well as the eventual changes in the redox state of the metal ions in the course of the reaction.

Experimental

All experiments were conducted at 37°C and run in duplicate.

Materials

Quercetin dihydrate (98%), $FeSO_4$, $7H_2O$ (99%), $FeCl_3$, $6H_2O$ (97%), $CuCl_2$, $2H_2O$ (99.9%), CuCl (99 + %), xylenol orange sodium salt, ferrozine (5,6-diphenyl-3-(2-pyridyl)-1,2,4 triazine-4′,4″-disulfonic acid sodium salt hydrate, 97%), bathocuproinedisulfonic acid disodium salt hydrate, butylated hydroxytoluene (BHT) and H_2O_2 (30%) were from Sigma-Aldrich. Ethylene diamine tetraacetic acid disodium dihydrate (EDTA) was from Normapur.

The buffers used in the experiments are a 0.2 M acetate buffer (pH 4.0) and a 0.01 M phosphate buffer (pH 7.4). Because of the poor solubility of quercetin, experiments in slightly acidic conditions (pH 5.0) were run in a 1:1 MeOH–acetate buffer mixture.

Analyses

Complexation and autoxidation reactions. The complexation and autoxidation processes were monitored using a HP 8453 diode-array spectrometer equipped with a magnetically stirred quartz cell (optical pathlength: 1 cm). The temperature in the cell was kept at 37°C by means of a thermostated bath. The 5×10^{-3} M solutions of metal ion were prepared in MeOH (Fe^{III}, Cu^{II}) or MeOH-0.2 M H_2SO_4 96:4 (Fe^{II}) or MeCN-0.2 M HCl 96:4 (Cu^{I}). The Fe^{II} and Cu^{I} solutions were prepared daily and checked for autoxidation using the proper colorimetric tests (see below).

To 2 ml of the pH 7.4 buffer solution placed in the spectrometer cell were successively added 20 µl of a freshly prepared 5×10^{-3} M solution of quercetin in MeOH and 10–100 µl of a freshly prepared 5×10^{-3} M solution of metal ion. Spectra were recorded every 0.5 s over 2 min (complexation) and every 30 s over 120 min (autoxidation). At pH 5, only complexation was investigated (spectra recorded every 5 s over 10 min). Eventually, the order of addition of quercetin and the metal ions into the buffer was reversed to outline the competition between quercetin and phosphate for the metal ions.

H_2O_2 titration [28]. The FOX2 reagent was prepared by mixing a solution of xylenol orange sodium salt (38 mg) and BHT (440 mg) in MeOH (450 ml) with a solution of $FeSO_4$, $7H_2O$ (49 mg) in 50 ml of 0.25 M H_2SO_4. Hence, the final composition of the FOX2 reagent was: 10^{-4} M xylenol orange, 4×10^{-3} M BHT, 25×10^{-3} M H_2SO_4 and 25×10^{-5} M $FeSO_4$, $7H_2O$ in 90% (v/v) MeOH. Aliquots (0.5 ml) of

RIGHTSLINK

Free Radic Res Downloaded from informahealthcare.com by Library of Health Sci-Univ of Il on 11/30/11
For personal use only.

a 10^{-4} M solution of quercetin (phosphate pH 7.4, 37°C) in the presence or absence of metal ion (1 equiv) were rapidly taken up, diluted into 1.5 ml of FOX2 reagent at room temperature, and stirred for 10 min. The samples were then transferred to the spectrometer cell for recording the absorbance at 592 nm (λ_{max} of the Fe^{III}-xylenol orange complex). In control experiments without quercetin, addition of Fe^{III}, Cu^{II} or Cu^{I} to the FOX2 reagent caused a time-dependent increase in A (592 nm) (attributed to slow metal exchange on the xylenol orange ligand) whose amplitude is in the order $Fe^{III} > Cu^{II} > Cu^{I}$. The corresponding values at 10 min must be subtracted. Corrections using Fe^{III} apply to any experiment involving iron ions, since Fe^{II} is rapidly autoxidized to Fe^{III} in the pH 7.4 phosphate buffer. Corrections using Cu^{I} apply to experiments using quercetin and Cu^{I} or Cu^{II}, since the latter is rapidly reduced to Cu^{I} by quercetin. Since distinct values are obtained for corrections with Cu^{I} and Cu^{II}, it is assumed that Cu^{I} autoxidation is negligible in the presence of the FOX2 reagent (Cu^{I} rapidly added to a FOX2 reagent-phosphate buffer (3:1) mixture). The H_2O_2 concentration is deduced from a calibration curve constructed by mixing the FOX2 reagent (1.5 ml) with aliquots (0.5 ml) of aqueous H_2O_2 solutions of known concentrations obtained by dilution of a 0.01 M solution (concentration determined from $\varepsilon(H_2O_2) = 40\ M^{-1}\,cm^{-1}$ at 240 nm). In those conditions, the apparent ε value of the Fe^{III}-xylenol orange complex at 592 nm was $65 \times 10^3\ M^{-1}\,cm^{-1}$.

Fe^{II} titration [29]. Aliquots (0.5 ml) of a 10^{-4} M solution of quercetin (phosphate pH 7.4, 37°C) in the presence of Fe^{II} or Fe^{III} (1 equiv) were rapidly taken up, diluted into 1.5 ml of an aqueous 10^{-3} M ferrozine solution at room temperature, and stirred for 10 min. The samples were then transferred to the spectrometer cell for recording the absorbance at 564 nm (λ_{max} of the Fe^{II}-ferrozine complex, $\varepsilon = 27{,}900\ M^{-1}\,cm^{-1}$).

Cu^{I} titration [30]. Aliquots (0.5 ml) of a 10^{-4} M solution of quercetin (phosphate pH 7.4, 37°C) in the presence of Cu^{II} or Cu^{I} (1 equiv) were rapidly taken up, diluted into 1.5 ml of an aqueous 10^{-3} M solution of bathocuproin disulfonate at room temperature, and stirred for 10 min. The samples were then transferred to the spectrometer cell for recording the absorbance at 480 nm (λ_{max} of the Cu^{I}-bathocuproin disulfonate complex, $\varepsilon = 13{,}900\ M^{-1}\,cm^{-1}$).

Data analysis. The curve-fittings of the absorbance vs time plots were carried out on a Pentium PC using the scientist program (MicroMath, Salt Lake City, UT). Beer's law and sets of differential kinetic equations (see text for the kinetic models used) with initial conditions on concentrations were input in the model. Curve-fittings were achieved through least square regression and yielded optimized values for the parameters (kinetic rate constants, molar absorption coefficients, stoichiometries). Standard deviations are reported.

HPLC-MS experiments. They were performed on a HP 1050 model equipped with a diode-array detector and coupled to a Micromass LCZ 4000 mass spectrometer. A C_{18} column (4.6 × 150 mm, 5 μm particle size) equipped with a pre-column (4.6 × 7.5 mm, 5 μm particle size) and kept at 25°C was used. The mobile phase (flow rate: 1.0 ml min^{-1}) was a linear gradient of acetonitrile and 0.05% aqueous HCO_2H with 5% MeCN at time 0 and 100% MeCN at 60 min. Mass spectra were recorded in the negative electrospray mode. The Masslynx program was used for data analysis.

Results and discussion

Autoxidation with no added metal ions

Autoxidation of quercetin (QH_2), which is barely detectable in a pH 5.0 acetate buffer, is significant in a pH 7.4 phosphate buffer (37°C). The spectral changes at 380 nm (quercetin consumption) and at 330 nm (formation of the quercetin autoxidation products QS) both obey an apparent first-order kinetics and give consistent values for the corresponding rate constant: $k_a = 57.5\ (\pm 0.3) \times 10^{-6}$ and $56.7(\pm 0.3) \times 10^{-6}\ s^{-1}$. Hence, the half-life of quercetin is roughly 3.4 h in these conditions. In addition, the following molar absorption coefficients can be estimated: $\varepsilon(QH_2,\ 380\ nm) = 18 \times 10^3\ M^{-1}\,cm^{-1}$, $\varepsilon(QS,\ 330\ nm) = 19 \times 10^3\ M^{-1}\,cm^{-1}$, $\varepsilon(QH_2, 330\ nm) = 1 \times 10^4\ M^{-1}\,cm^{-1}$. From the literature and our previous works [31–35], we assume that the autoxidation products (QS) detectable at 330 nm result from solvent addition (S=H_2O or MeOH) on the *p*-quinonemethide (Q) formed by two-electron oxidation of quercetin (Scheme 1, QS stands for QMeOH, QH_2O and QH_2OMeOH taken collectively). This can be confirmed by HPLC-MS analysis (Table I). It can be noted that even the low MeOH content of the neutral buffer used in this work was sufficient for the detection of *p*-quinonemethide-MeOH adducts (QMeOH, QH_2OMeOH). In the course of quercetin autoxidation, an apparent zero-order formation of H_2O_2 with $R(H_2O_2) = 3 \times 10^{-10}\ M\,s^{-1}$ (quercetin concentration = 10^{-4} M) could be evidenced over 3 h. Hence, after 3 h, it can be estimated that *ca.* 3 μM H_2O_2 has accumulated whereas almost 50 μM quercetin has been consumed.

RIGHTSLINK

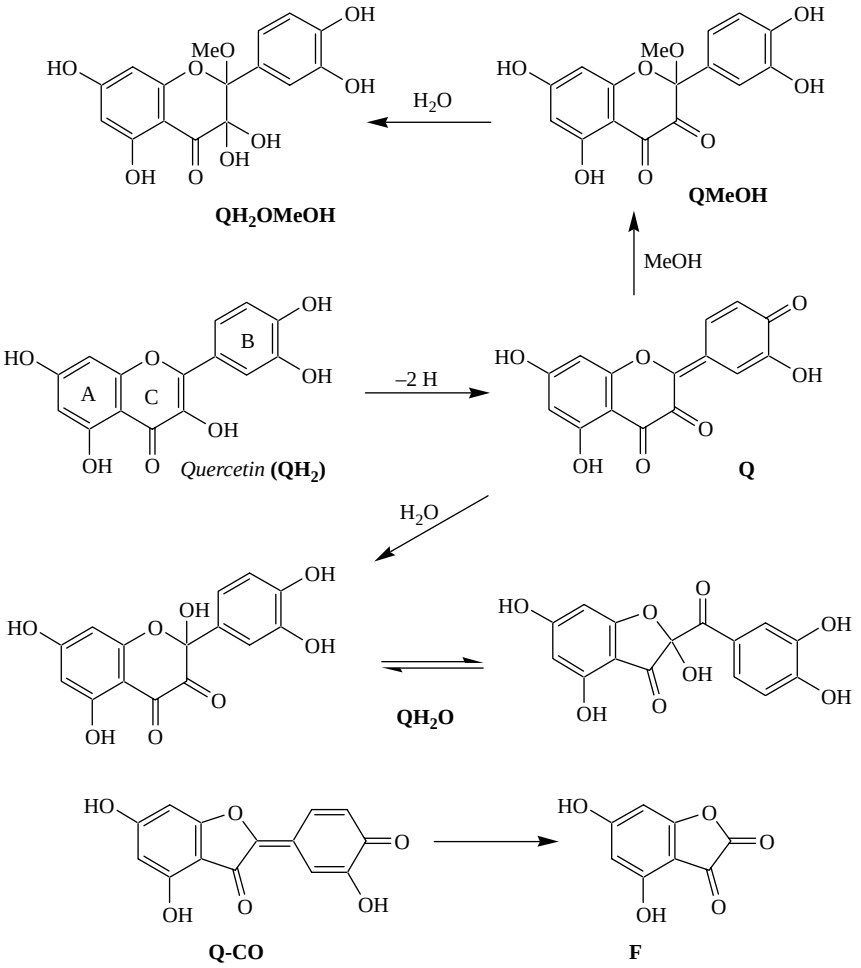

Scheme 1.

Although, it may be tempting to consider the first step of quercetin autoxidation as a direct electron transfer from quercetin (mainly, a dianion at pH 7.4 [36]) to dioxygen, it must be noted that the corresponding thermodynamics is quite unfavourable since the redox potential of the $QH^{\cdot}/QH_2$ and O_2(dissolved)/$O_2^{\cdot-}$ couples at pH 7 are 0.33 [37] and -0.16 V, respectively. In fact, the combination of unfavourable thermodynamics and spin restrictions (O_2 is a spin 1 molecule) should make the direct electron transfer a very slow process [19]. Hence, catalysis by unidentified metal traces must operate [20]. In the presence of quercetin and its oxidation products, these metal traces could efficiently decompose H_2O_2 (formed during quercetin autoxidation), thereby preventing its accumulation.

Iron-quercetin complexation at pH 5

The spectral changes following the addition of iron ions to a pH 5 acetate buffer containing quercetin can be ascribed to pure complexation. Indeed, no increase

Table I. HPLC-MS data for the autoxidation of quercetin (10^{-4} M) with or without added Fe^{III} (1–2 equiv, added last) in 0.01 M phosphate buffer–MeOH (95:5) (pH 7.4, 37°C). Analysis after 15 h (no added Fe^{III}) or 1–6 h (+Fe^{III}).

Retention time/min	*m/z*[*]	λ_{max}/nm	Structure[†]
14.0	317, 299, 261, 255, 199, 179, 163, 137	292	QH_2O
16.0	331, 299, 271, 261, 217, 199, 187, 137	292	QMeOH
19.1[‡]	349, 331, 299, 271	292	QH_2OMeOH
22.8	301, 179, 151	254, 370	QH_2

[*] Molecular mass of possible structures and fragments: $QH_2OMeOH = 350$, $QMeOH = 332$, $QH_2O = 318$, $Q = 300$, $Q–CO = 272$, $QH_2O–2CO = 262$, $Q–CO_2 = 256$, $Q–CO = 272$, $QH_2O–2CO–CO_2 = 218$, $Q–2CO–CO_2 = 200$, $F = 180$, $F–O = 164$, $F–CO = 152$, dihydroxybenzaldehyde = 138. [†] See Scheme 1 quercetin (QH_2), *p*-quinonemethide-water adduct (QH_2O), *p*-quinonemethide-MeOH adduct (QMeOH), *p*-quinonemethide-water-MeOH adduct (QH_2OMeOH). [‡] Detected in the absence of added Fe^{III}, only.

Free Radic Res Downloaded from informahealthcare.com by Library of Health Sci-Univ of Il on 11/30/11
For personal use only.

RIGHTSLINK

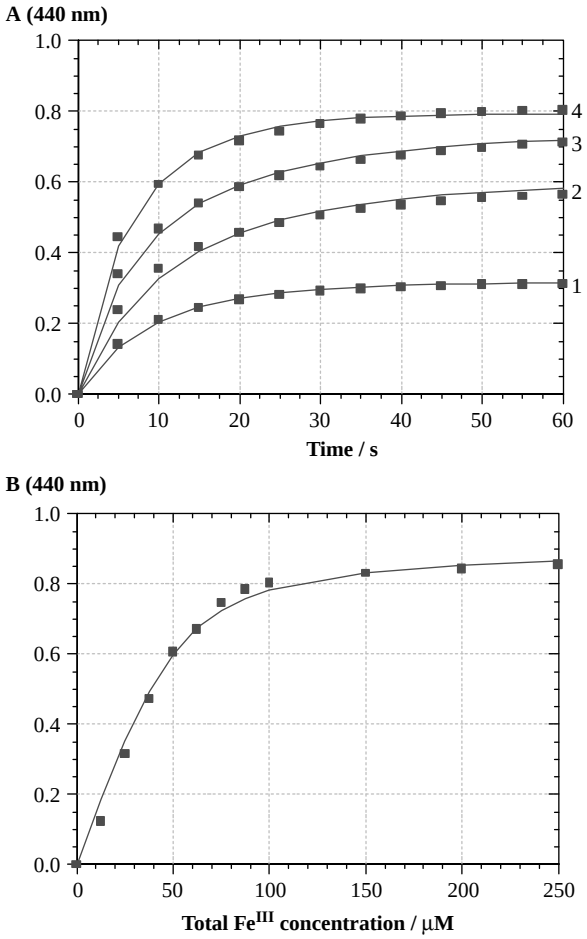

Figure 1. Complexation of quercetin (5×10^{-5} M) by Fe^{III} in a 1:1 0.2 M acetate buffer-MeOH mixture (pH 5, 37°C). (Part A) A(440 nm) vs time curves: Fe^{III}/quercetin molar ratio = 0.5(1), 1.0(2), 1.5(3), 2(4). (Part B) A(440 nm) vs total Fe^{III} concentration plot. The solid lines are the results of the curve-fitting procedures (see text).

in the absorbance around 300 nm that would point to oxidation can be detected. The appearance of a broad absorption band around 440 nm is ascribed to metal complexes and reaches a maximal intensity over *ca.* 1 min (Figure 1). For iron/quercetin molar ratios higher than two, precipitation was observed at the end of the kinetic run, especially with Fe^{III}. Plateau values of A(440 nm) can be used to estimate the stability constant K_1 of the complex (noted QM). Assuming 1:1 binding, the following equations can be easily derived and used in the fitting of the $A_{plateau}$(440 nm) vs total metal concentration curve (ε_1, molar absorption coefficient of QM; $[M]$, free metal concentration; M_t, total metal concentration; c, total quercetin concentration, no significant absorption for both M and QH_2 at 440 nm) (Figure 1):

$$A_{plateau} = \varepsilon_1 \frac{K_1[M]c}{1 + K_1[M]}$$

$$[M] = \frac{M_t}{1 + \frac{K_1 c}{1 + K_1[M]}}$$

This procedure allows to ensure that the complexation equilibrium is reached while avoiding autoxidation and precipitation (which ultimately proceeds at the highest Fe^{III} concentrations studied). Calculations with Fe^{III} give: $K_1 = 119\ (\pm 25) \times 10^3\ M^{-1}$, $\varepsilon_1 = 18{,}000\ (\pm 480)\ M^{-1}\,cm^{-1}$ ($r = 0.997$). In the case of Fe^{II}, one obtains: $K_1 = 78\ (\pm 21) \times 10^3\ M^{-1}$, $\varepsilon_1 = 18{,}800\ (\pm 800)\ M^{-1}\,cm^{-1}$ ($r = 0.993$). The increase in A(440 nm) can also be fitted against a simple kinetic model assuming reversible second-order metal complexation of quercetin (QH_2) to form complex QM (first-order rate constant k_1). Hence, the following rate laws are used in the curve-fitting procedure:

$$-\frac{d}{dt}[QH_2] = -\frac{d}{dt}[M] = \frac{d}{dt}[QM]$$

$$= k_1[QH_2][M] - \frac{k_1}{K_1}[QM]$$

Rate constant k_1 and binding constant K_1 are the adjustable parameters, the molar absorption coefficients of the metal complexes being set at their values deduced from the analysis of the $A_{plateau}$ vs M_t curve (see above). The corresponding values are collected in Table II. Both procedures give consistent K_1 values. As expected, quercetin has a stronger affinity for Fe^{III} than for Fe^{II}. The stronger Fe^{III}-quercetin binding is essentially reflected in a faster association. According to the literature [38], Fe^{III} could be oxidizing enough

Table II. Complexation of quercetin (5×10^{-5} M) by Fe^{II} and Fe^{III} in a 1:1 0.2 M acetate buffer–MeOH mixture (pH 5, 37°C). Spectroscopic monitoring at 440 nm (metal complexes) over 2 min. Molar absorption coefficients of the complexes set at 18,000 and 18,800 $M^{-1}\,cm^{-1}$ for Fe^{III} and Fe^{II}, respectively (see text).

Fe conc./μM	$k_1(Fe^{III})/M^{-1}\,s^{-1}$	$10^{-3}K_1(Fe^{III})/M^{-1}$	$k_1(Fe^{II})/M^{-1}\,s^{-1}$	$10^{-3}K_1(Fe^{II})/M^{-1}$
50	1222(±22)	117.2(±0.8)	1067(±41)	36.6(±0.8)
75	1203(±40)	129.0(±4.2)	–	–
100	1510(±43)	133.7(±7.3)	866(±33)	79.6(±2.4)
125	–	–	982(±26)	77.3(±2.5)
150	1448(±12)	113.3(±2.5)	918(±31)	75.5(±5.1)
200	1160(±36)	107(±11)	844(±34)	71.1(±6.4)
250	1218(±10)	96.5(±2.6)	814(±36)	57.5(±6.7)

Free Radic Res Downloaded from informahealthcare.com by Library of Health Sci-Univ of Il on 11/30/11
For personal use only.

RIGHTSLINK

at pH 5.0 to be reduced to Fe^{II} by quercetin (a 1:1 stoichiometry was reported for this reaction in a pH 5.5 acetate buffer). HPLC analysis actually allowed us to detect quercetin oxidation products QS. However, over the period of spectroscopic monitoring of iron-quercetin complexation (1–2 min), no significant development of absorption around 300 nm that would be typical of QS can be noted. We thus assume that quercetin oxidation is negligible under these conditions and that the data reported in Table II only refer to complexation.

Iron-quercetin complexation at pH 7.4

At pH 7.4, Fe-quercetin complexation is much faster than at pH 5.0 (Figure 2). This must reflect the fact that competition between protons and metal ions for the quercetin-binding site is more in favour of complexation. For Fe/quercetin molar ratios higher than 1, the fast increase in A(460 nm) is followed by a slower increase (Figure 2, curve 2A). Hence, the whole A(460 nm) vs time curves could not be kinetically analyzed within the assumption of simple 1:1 binding. On the other hand, the hypothesis of two quasi-irreversible binding processes successively yielding complex QM (rate constant k_1, molar absorption coefficient ε_1) and complex QM_2 (rate constant k_2, molar absorption coefficient ε_2) gave quite satisfactory curve-fittings. The corresponding values of the optimized parameters are reported in Table III. For Fe/quercetin molar ratios lower than 1, reversibility in QM formation must be assumed. Good curve-fittings are obtained by using an estimate for ε_1 from experiments at Fe/quercetin molar ratios higher than 1, k_1 and K_1 being the adjustable parameters. The corresponding binding constants can be estimated: $K_1(Fe^{II}\text{-quercetin}) = 4 \times 10^5$, $K_1(Fe^{III}\text{-quercetin}) = 16 \times 10^3\ M^{-1}$. The formation of 1:1 and 2:1 Fe^{III}-quercetin complexes has already been reported in the literature from potentiometric titrations in aqueous solutions [36]. Indeed, quercetin displays up to three distinct sites for metal binding: the catechol nucleus (1,2-dihydroxybenzene, B-ring), a α-hydroxyketo group (C-ring) and a β-hydroxyketo group (A- and C-rings). However, comparison between flavones possessing only one of those metal binding sites clearly shows that the catechol nucleus by far displays the highest affinity for Fe^{III}, especially in neutral conditions [39].

In the case of Fe^{III}, the complexation kinetics is deeply affected by the order of addition of the reagents (Figure 2). For instance, when quercetin is added to a solution of Fe^{III} in the phosphate buffer, the Fe^{III}-quercetin complexation is relatively slow because quercetin must displace tightly bound phosphate ligands for the binding to proceed. As a result, the apparent thermodynamics of complexation is less favourable ($K_1(Fe^{III}\text{-quercetin}) = 3–4 \times 10^3\ M^{-1}$).

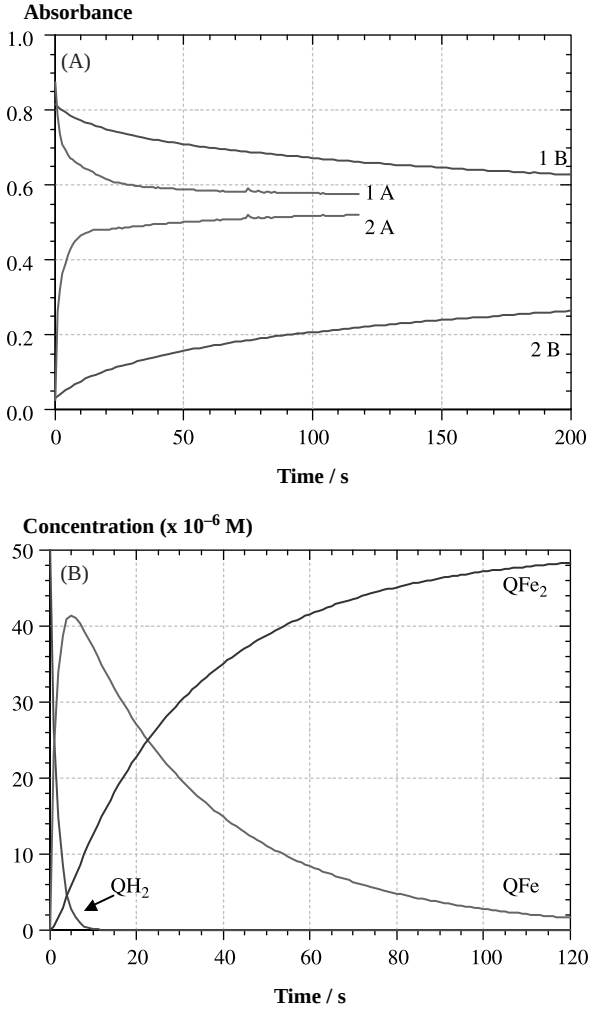

Figure 2. Complexation of quercetin (5×10^{-5} M) by Fe^{III} (5 equiv) in a 0.01 M phosphate buffer (pH 7.4, 37°C). (Part A) absorbance vs time curves. (Curves 1A and B) detection at 380 nm. (Curves 2A and B) detection at 460 nm (curves 1A, 2A: Fe^{III} added last, curves 1B, 2B: quercetin added last). (Part B) concentration vs time curves (Fe^{III} added last).

By contrast, when Fe^{III} (weakly bound to MeOH molecules) is added to a solution of quercetin in the phosphate buffer, the Fe^{III}-quercetin complexation appears faster, probably because it successfully competes with iron–phosphate complexation under these conditions. Anyway, quercetin-Fe^{III} binding remains slower than quercetin-Fe^{II} binding because competition between quercetin and phosphate ions is more severe in the case of Fe^{III} than in the case of Fe^{II}. In the kinetic analysis (Table III), the kinetics of iron–phosphate complexation is not explicitly taken into account so that the corresponding rate constants must be considered as apparent (buffer-dependent) parameters. In the case of Fe^{II}, the influence of the order of addition of the reagents cannot be rigorously studied because autoxidation of Fe^{II} is quite fast in a neutral phosphate buffer due to the stronger interaction of the phosphate ions with Fe^{III} [29]. In fact, in those conditions, Fe^{II} titration in the absence or presence

Free Radic Res Downloaded from informahealthcare.com by Library of Health Sci-Univ of Il on 11/30/11
For personal use only.

RIGHTSLINK

Table III. Complexation of quercetin (5×10^{-5} M) by Fe^{II} and Fe^{III} in a 0.01 M phosphate buffer (pH 7.4, 37°C). Spectroscopic monitoring at 460 nm (metal complexes) over 2 min.

Fe conc./μM	$k_1/M^{-1}s^{-1}$, K_1/M^{-1}	$\varepsilon_1/M^{-1}cm^{-1}$	$k_2/M^{-1}s^{-1}$	$\varepsilon_2/M^{-1}cm^{-1}$
Fe^{II}, 37.5⋆	8560(±210) $37.2(\pm 0.6) \times 10^4$	10^4	–	–
50⋆	9130(±290) $45.5(\pm 1.0) \times 10^4$	10^4	–	–
75	12100(±100)	9600(±20)	743(±64)	10600(±20)
100	10760(±100)	9400(±30)	1901(±82)	11030(±10)
125	7209(±51)	9910(±30)	1732(±56)	11020(±10)
150	11290(±450)	9120(±130)	1875(±117)	11350(±10)
175	4808(±66)	10710(±60)	879(±71)	11510(±10)
200	9060(±220)	10180(±90)	1505(±76)	11920(±10)
Fe^{III}, 50⋆	1912(±26) $16.1(\pm 0.1) \times 10^3$	6300	151(±4)	8500
75⋆	1577(±18) $15.6(\pm 0.1) \times 10^3$	6300	88(±2)	8500
125	3355(±41)	6300(±20)	56(±15)	8800(±450)
150	3062(±33)	7130(±20)	158(±14)	8520(±50)
175	4160(±140)	6340(±60)	298(±18)	8410(±20)
200	3000(±70)	6270(±40)	155(±8)	8640(±30)
225	1809(±20)	7150(±20)	53(±6)	8760(±90)
250	2740(±90)	8330(±70)	176(±18)	9920(±30)
Fe^{III}, 150⋆,†	91.4(±1.1) 3577(±65)	6300	63.7(±1.3)	8500
200⋆,†	87(±1) 3938(±90)	6300	50.7(±1.2)	8500
250⋆,†	63.2(±0.5) 3320(±57)	6300	36.5(±0.6)	8500

⋆ Reversible 1:1 binding assumed (binding constant K_1). † Quercetin added last.

of quercetin shows that most Fe^{II} is converted into Fe^{III} within the first minutes following addition of Fe^{II} to the phosphate buffer (Figure 3). Quercetin-Fe^{II} binding only provides marginal protection to Fe^{II} against autoxidation. Hence, experiments in which quercetin is added to a solution of Fe^{II} in the phosphate buffer were not considered. Despite the fast autoxidation of Fe^{II}, the kinetic data obtained when iron is added last are significantly distinct for Fe^{II} and Fe^{III}. Hence, in the experiment with Fe^{II}, we may assume that most of the iron is in the Fe^{II} state during the time period used for spectral measurements (2 min).

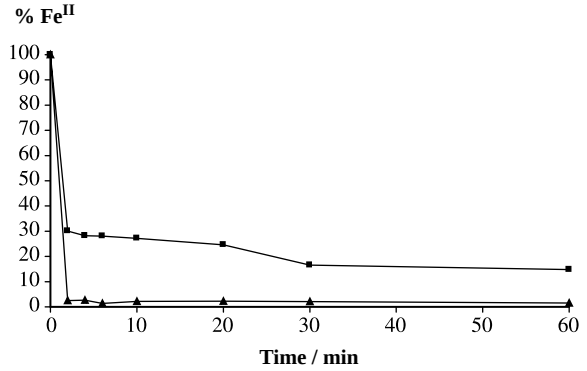

Figure 3. Time-dependence of the Fe^{II} concentration (10^{-4} M) in a 0.01 M phosphate buffer (pH 7.4, 37°C) in the absence (▲) or presence of quercetin (10^{-4} M) (■).

Copper-quercetin complexation at pH 7.4

When Cu^{II} is added to a solution of quercetin (Cu^{II}/quercetin molar ratio ≤ 1), a fast monotonous increase in $A(460\,nm)$ (Figure 4) which is in agreement with previous reports [38]. A plot of the $A_{max}(460\,nm)$ vs total metal complexation can be fitted assuming 1:1 binding to give: $K_1 = 180\ (\pm 34) \times 10^3\,M^{-1}$, $\varepsilon_1 = 15{,}780(\pm 380)\,M^{-1}\,cm^{-1}$ ($r = 0.9995$, data not shown). However, at Cu^{II}/quercetin molar ratios lower than 1, the $A(460\,nm)$ vs time curves could not be analyzed within this simple hypothesis even when taking into account reversibility (ε_1 set at $15{,}780\,M^{-1}\,cm^{-1}$). We just mention that correct curve-fittings are obtained by assuming a quasi-irreversible 1:1 binding to form complex QM (second-order rate constant k_1, molar absorption coefficient ε_1) followed by an apparent first-order conversion of QM into QM′ (rate constant k_1', molar absorption coefficient ε_1') (Table IV). A possible interpretation could be a rearrangement within the copper coordination sphere promoted by slow phosphate binding. However, redox processes cannot be excluded although no significant increase in $A(330\,nm)$ that would point to the formation

Free Radic Res Downloaded from informahealthcare.com by Library of Health Sci-Univ of Il on 11/30/11
For personal use only.

RIGHTSLINK

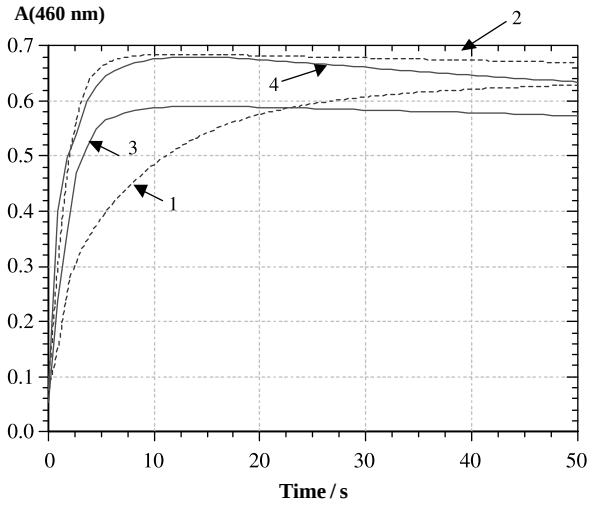

Figure 4. Complexation of quercetin (5×10^{-5} M) by Cu^{II} (dash lines, curve 1:1 equiv, curve 2:2 equiv) and Cu^{I} (solid lines, curve 3:1 equiv, curve 4:2 equiv) in a 0.01 M phosphate buffer (pH 7.4, 37°C).

of quercetin oxidation products, is observed. At Cu^{II}/quercetin molar ratios higher than 1, the first part of the A(460 nm) vs time curves (slow decay not considered) can be treated within the assumption of a simple irreversible 1:1 binding. The corresponding rate constants are in reasonable agreement with those deduced from a kinetic analysis at 380 nm (absorption maximum for quercetin) (Table IV).

In the case of the Cu^{I}-quercetin complexation, the building-up of A(460 nm) is even faster than with the other metal ions investigated (Figure 4). Assuming an irreversible 1:1 binding, the kinetic analysis of the A(460 nm) vs time curves over the first 15 s allows to obtain an estimate for the corresponding rate constant: k_1 *ca.* $10^4\,M^{-1}\,s^{-1}$ (Table IV). After this fast binding step, a slow decay of A(460 nm) can be observed (Figure 4), which suggests either the rearrangement of the primary complex (kinetic product) into a more stable one (thermodynamic product) or the onset of quercetin autoxidation (see below).

Copper-quercetin complexation probably occurs via the 4-keto group of the C-ring with additional involvement of the O3–H or O5–H group [38]. Indeed, the copper-induced bathochromic shift of the low-energy absorption band of quercetin (*ca.* 50 nm for a quercetin-copper ion molar ratio of 1) is larger by more than 30 nm than that induced by the iron ions (binding at the catechol site [39]).

In summary, addition of iron or copper ions to a solution of quercetin in a neutral phosphate buffer is followed by fast metal-quercetin complexation. The apparent second-order rate constants of 1:1 binding (k_1) are in the order: Cu^{I} (*ca.* $1 \times 10^4\,M^{-1}\,s^{-1}$) $> Cu^{II}$, Fe^{II} ($5–10 \times 10^3\,M^{-1}\,s^{-1}$) $> Fe^{III}$ ($2–4 \times 10^3\,M^{-1}\,s^{-1}$). The binding kinetics is complicated by additional 2:1 metal-quercetin complexation (Fe ions in excess) and rearrangement of the primary complexes into more stable complexes (copper ions).

Autoxidation in presence of iron ions at pH 7.4

When the spectral changes following Fe addition are monitored over 2 h, a combination of chemical processes can be observed: during the first minutes, the spectral changes essentially reflect complexation since no increase in the absorbance at 330 nm typical of quercetin oxidation products (QS) is detected. Then, the continuous slow increase in A(330 nm) and decrease in A(380 nm) is indicative of quercetin autoxidation (Figures 5 and 6). However, monitoring at 460 nm (metal complexes) points to a biphasic process. Indeed, following the fast complexation step, A(460 nm) keeps increasing more slowly and either reaches a stable plateau value (iron/quercetin molar ratio ≤ 1, Figure 5) or tends to decrease very slowly (iron/quercetin molar ratio > 1, Figure 6). A more detailed kinetic analysis can be proposed based on the simplification that metal complexation is fast

Table IV. Complexation of quercetin (5×10^{-5} M) by copper ions in a 0.01 M phosphate buffer (pH 7.4, 37°C). Spectroscopic monitoring at 460 nm (metal complexes) over 2 min.

Cu conc./μM	$k_1/M^{-1}s^{-1}$	$\varepsilon_1/M^{-1}cm^{-1}$	$10^3 k'_1\,s$	$\varepsilon'_1/M^{-1}cm^{-1}$
Cu^{II}, 12.5	7840(±480)	8900(±250)	45(±3)	13450(±50)
25	5930(±570)	8540(±440)	40(±3)	13740(±60)
37.5	7890(±320)	10290(±160)	26(±4)	12210(±80)
50*	3810(±60)	12000(±30)	–	–
	2920(±30)	8050(±20)	–	–
100(0–15 s)*	6140(±400)	12410(±150)	–	–
	5620(±370)	7190 (±160)	–	–
125(0–15 s)*	6650(±100)	14720(±30)	–	–
	5410 (±320)	7900 (±110)	–	–
Cu^{I}(0–15 s)				
75	8990(±490)	12610(±150)	–	–
100	8690(±370)	12040(±80)	–	–

* The second set of parameters is gained from monitoring at 380 nm.

Free Radic Res Downloaded from informahealthcare.com by Library of Health Sci-Univ of Il on 11/30/11
For personal use only.

RIGHTSLINK

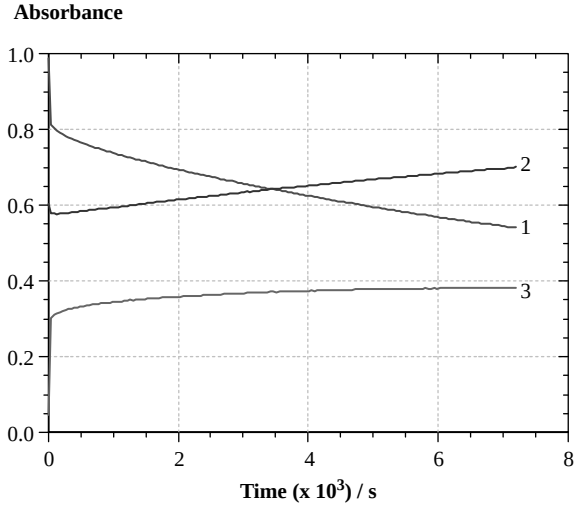

Figure 5. Autoxidation of quercetin (5×10^{-5} M) after addition of Fe^{III} (1 equiv) in a 0.01 M phosphate buffer (pH 7.4, 37°C). (Curve 1) detection at 380 nm. (Curve 2) detection at 330 nm. (Curve 3) detection at 460 nm.

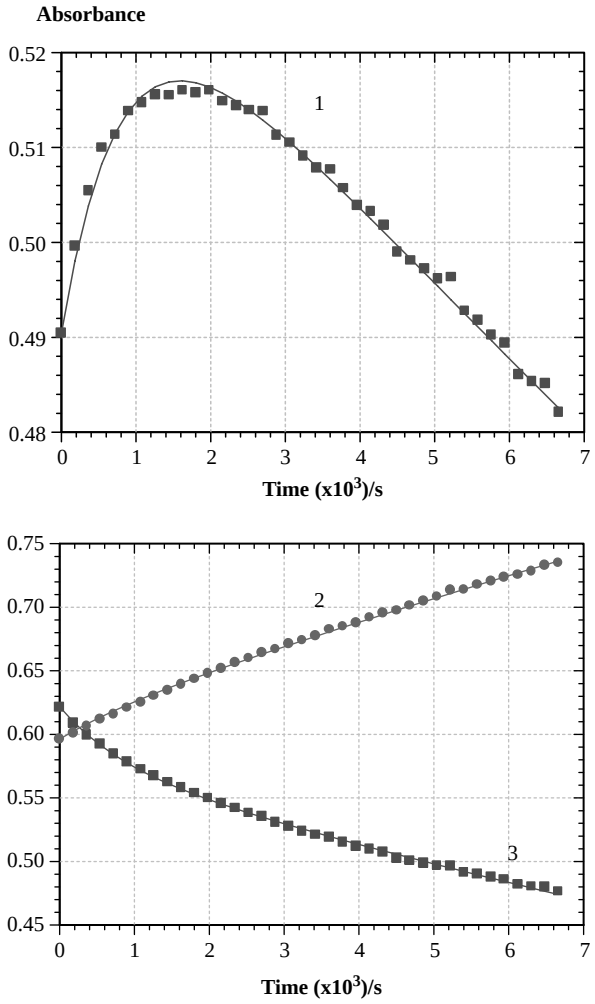

Figure 6. Autoxidation of quercetin (5×10^{-5} M) after addition of Fe^{III} (3 equiv) in a 0.01 M phosphate buffer (pH 7.4, 37°C). (Curve 1) detection at 460 nm. (Curve 2) detection at 330 nm. (Curve 3) detection at 380 nm. The solid lines are the results of the curve-fitting procedures.

and quasi-irreversible. Thus, at the end of the fast step (1–3 min), the quercetin and metal complex concentrations are, respectively approximated to $c - M_t$ and M_t (M_t: total metal concentration, c: total quercetin concentration) when $c > M_t$, and 0 and c when $M_t > c$. Those concentrations are used as initial conditions for the curve-fitting procedures dealing with autoxidation (monitoring over 2 h following the fast complexation step). For Fe^{III}/quercetin molar ratios higher than 1, the A(460 nm) vs time curves can be interpreted by assuming the relatively fast conversion of the metal complexes (QM and QM_2 taken collectively) into a first product P_1 absorbing at 460 nm (apparent first-order rate constant k'_1) which slowly decays into a final product P_2 that does not absorb at 460 nm (apparent first-order rate constant k'_2). Then, the simultaneous fitting of the A(380 nm) and A(330 nm) vs time curves with k'_1 held to its value deduced from the kinetic analysis at 460 nm yields refined values for the rate constant k'_2 (Figure 6, Table V). With Fe^{II} in excess, the reverse procedure gave better results, i.e. simultaneous fitting of the A(380 nm) and A(330 nm) vs time curves to extract values for k'_1 and k'_2 followed by fitting of the A(460 nm) vs time curve with k'_1 held constant to obtain a second estimate of k'_2 (Table VI). Product P_1 displays absorption bands at 460 and 380 nm. Its absorption at 330 nm is *ca.* twice as low as for product P_2, which on the other hand does not absorb at 460 and 380 nm. It is thus reasonable to assume that P_1 is a metal complex steming from rearrangement in the coordination sphere of complex QM (QM_2), as already observed in the investigation of copper-quercetin complexation, and that P_2 is the mixture of quercetin oxidation products (QS) evidenced by HPLC-MS and displaying a typical absorption band at 330 nm in neutral aqueous solution. The corresponding molar absorption coefficient is *ca.* $2 \times 10^4\ M^{-1}\,cm^{-1}$ (as estimated in quercetin autoxidation with no metal added, see above) although larger values are obtained in the curve-fittings dealing with the most concentrated solutions of metal ions because of the weak (uncorrected) absorption of the free metal ion at 330 nm.

For Fe/quercetin molar ratios lower than 1, free quercetin is still present in the solutions so that the direct autoxidation mechanism that does not involve complex QM as an intermediate must be taken into account for a correct fitting. Satisfactorily, the corresponding rate constant is in good agreement with that deduced from the experiment with no metal added (see above) (Tables V and VI). However, it can be noted that A(460 nm) does not significant decay for Fe/quercetin molar ratios equal to 0.5 and 1 (in Tables V and VI, the corresponding k'_2 values

Free Radic Res Downloaded from informahealthcare.com by Library of Health Sci-Univ of Il on 11/30/11
For personal use only.

RIGHTSLINK

Table V. Autoxidation of quercetin (5×10^{-5} M) in the presence of Fe^{III} in a 0.01 M phosphate buffer (pH 7.4, 37°C). Without EDTA, the spectral changes occurring during 3 min following the addition of Fe^{III} (pure complexation) are not considered in the calculations. At time zero, all quercetin is assumed to be bound to Fe^{III}, except for 25 μM Fe^{III} (50% binding). Values in brackets are the wavelengths of detection (in nm).

Fe^{III} conc./μM*	10^5 k'_1 s	10^5 k'_2 s	ε'_1, ε'_2/$M^{-1}cm^{-1}$
25(460)	39(±1)	–	7950(±10), 0
25(380)	39	4.90(±0.02)	11630, 0
(330)†		4.90‡	12170, 16680
50(460)	54(±1)	–	6730(±10), 0
50(380)	54	4.11(±0.02)	13270, 0
(330)			12400, 21090
100(460)	69(±2)	1.25(±0.01)	9360(±10), 0
100(380)	69	3.05(±0.02)	10920, 0
(330)			11930, 24830
150(460)	119(±2)	1.67(±0.02)	10380(±10), 0
150(380)	119	2.97(±0.01)	11270, 0
(330)			12530, 26410
200(460)	139(±3)	1.99(±0.01)	10810(±10), 0
200(380)	139	2.62(±0.01)	11580, 0
(330)			14200, 30860
250(460)	181(±3)	2.11(±0.01)	11080(±10), 0
250(380)	181	2.43(±0.01)	11640, 0
(330)			14990, 32380
Fe^{III} conc./μM¶	k'_1/$M^{-1}s^{-1}$	10^5 k'_2/s^{-1}	ε'_1, ε'_2/$M^{-1}cm^{-1}$
25(380)	12.7(±4.8)	31(±7)	16660, 0
(330)			17100, 24570
50(380)	5.8(±0.3)	22.6(±1.0)	13280, 0
(330)			19290, 24100
100(380)	2.4(±0.3)	19.5(±2.0)	10680, 0
(330)			25720, 28440
150(380)	1.4(±0.4)	17.7(±3.5)	9150, 0
(330)			30940, 33430

* No EDTA. † Autoxidation of QM and free quercetin. ‡ Rate constant for the autoxidation of free quercetin (set equal to k'_2 for fitting). ¶ With EDTA (0.5 mM).

Free Radic Res Downloaded from informahealthcare.com by Library of Health Sci-Univ of Il on 11/30/11
For personal use only.

deduced from the kinetic analysis at 460 nm are either zero or very small) while autoxidation is well evidenced by the increase in A(330 nm) and decrease in A(380 nm) (Figure 5). These discrepancies point to the limits of our kinetic approach and suggest that iron-quercetin binding is reversible under such conditions and that the spectral changes essentially reflect autoxidation of free quercetin.

The apparent rate constant k'_1 increases monotonously with the Fe^{III} concentration in the range $4–18 \times 10^{-4}\,s^{-1}$. No such clear dependence could be observed with the Fe^{II}-initiated process (k'_1 in the range $3–9 \times 10^{-4}\,s^{-1}$). The k'_2 values ($1–4 \times 10^{-5}\,s^{-1}$) display no clear dependence on the Fe concentration or on the Fe redox state. These parameters are proposed to measure the sensitivity of the iron–quercetin complexes toward autoxidation in a neutral phosphate buffer. In comparison with the autoxidation of quercetin with no added metal ion (k_a *ca.* $6 \times 10^{-5}\,s^{-1}$), it can be concluded that the iron complexes of quercetin are less reactive than free quercetin toward dioxygen. In other words, iron complexation weakly protects quercetin against autoxidation. The autoxidation kinetics of the iron-quercetin complexes is essentially independent of the iron redox state. It can thus be proposed that the Fe^{II}-quercetin complexes are rapidly converted in Fe^{III}-quercetin complexes in agreement with the observation that Fe^{II} does not accumulate in the course of quercetin autoxidation (Figure 3).

When Fe^{III} or Fe^{II} is added to a solution of quercetin in the presence of EDTA (EDTA/quercetin molar ratio = 10), no absorption band above 400 nm can be detected. Clearly, EDTA-bound iron is no longer available to strongly complex quercetin. Under such non-complexing conditions, autoxidation is weakly accelerated by iron. Excellent curve-fittings of both the A(380 nm) and A(330 nm) vs time curves (Figure 7) could be achieved within the hypothesis of a two-step process involving the formation of a labile complex QM (second-order rate constant k'_1, absorption at 380 nm) that reacts with dioxygen to yield QS (first-order rate constant k'_2, no absorption at 380 nm). The k'_1 and k'_2 values are not significantly dependent on the Fe redox state (Tables V and VI). Parameter k'_1 tends to decrease when the total metal concentration increases, probably because of unaccounted reversibility in QM formation. Parameter k'_2, which is approximately constant and independent of the total metal concentration, can be taken as a measure of the

RIGHTSLINK

Table VI. Autoxidation of quercetin (5×10^{-5} M) in the presence of Fe^{II} in a 0.01 M phosphate buffer (pH 7.4, 37°C). Without EDTA, the spectral changes occurring during 90 s following the addition of Fe^{II} (pure complexation) are not considered in the calculations. At time zero, all quercetin is assumed to be bound to Fe^{II}, except for 25 μM Fe^{III} (50% binding). Values in brackets are the wavelengths of detection (in nm).

Fe^{II} conc./μM*	10^5 k'_1 s	10^5 k'_2 s	ε'_1, ε'_2/$M^{-1}cm^{-1}$
25(460)	171(±7)	0.42(±0.01)	12800(±10), 0
25,(380)	171	0.37(±0.15)	9070, 0
(330)†		6.3(±0.1)‡	7900, 24010
50(460)	71(±1)	–	7140(±10), 0
50(380)	71	4.00(±0.01)	13570, 0 11660, 21010
(330)			
100(460)	90	2.23(±0.02)	10380(±10), 0
100(380)	90(±3)	2.56(±0.02)	12490, 0
(330)			12370, 27060
150(460)	39	2.51(±0.01)	10150(±10), 0
150(380)	39(±1)	2.21(±0.02)	9950, 0
(330)			12900, 28040
200,(460)	44	3.10(±0.03)	10780(±10), 0
200(380)	44(±1)	2.40(±0.02)	10090, 0
(330)			13760, 29640
250(460)	31	2.98(±0.03)	10740(±10), 0
250(380)	31(±2)	1.38(±0.01)	10290, 0
(330)			17380, 43260
Fe^{II} conc./μM¶	k'_1/$M^{-1}s^{-1}$	10^5 k'_2/s^{-1}	ε'_1, ε'_2/$M^{-1}cm^{-1}$
25(380)	10.6(±3.0)	25(±4)	14470, 0 15650, 22120
(330)			
50(380)	5.4(±0.3)	19.1(±0.8)	13820, 0 20080, 25370
(330)			
100(380)	2.6(±0.3)	21.9(±2.2)	11340, 0 23430, 26770
(330)			
150(380)	1.8(±0.4)	24.6(±5.5)	11970, 0
(330)			28330, 28840

* No EDTA. † Autoxidation of QM and free quercetin. ‡ Rate constant for the autoxidation of free quercetin. ¶ With EDTA (0.5 mM).

sensitivity of quercetin to autoxidation initiated by EDTA-iron. From its value ($2–3 \times 10^{-4}\,s^{-1}$), it can be concluded that EDTA-iron accelerates quercetin autoxidation by a factor 3–4 only.

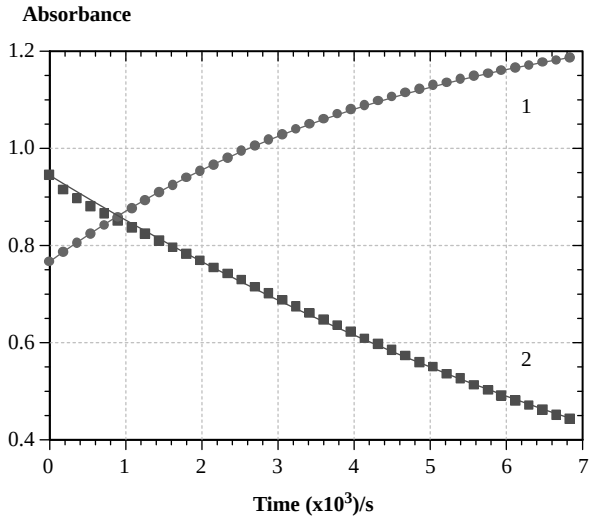

Figure 7. Autoxidation of quercetin (5×10^{-5} M) after addition of Fe^{III} (2 equiv) in a 0.01 M phosphate buffer (pH 7.4, 37°C) containing EDTA (5×10^{-4} M). (Curve 1) detection at 330 nm. (Curve 2) detection at 380 nm. The solid lines are the results of the curve-fitting procedures.

When quercetin autoxidation takes place in the presence of added Fe^{II} with or without EDTA, the ROS possibly formed during fast Fe^{II} autoxidation do not seem to significantly accelerate the consumption of quercetin, which in both cases does not appear faster than the corresponding process in the presence of added Fe^{III} (Tables V and VI).

Taken together, the data about quercetin autoxidation in a neutral iron-containing phosphate buffer suggest that iron ions accelerate the reaction in non-complexing conditions, only. The redox potential of the Fe^{III}/Fe^{II} couple is strongly pH-dependent because of the successive deprotonations of Fe^{3+}-bound water molecules in the pH range 2–4. Hence, $E^0(Fe^{III}/Fe^{II})$ drops from 0.77 V at pH 0 to 0.11 V at neutral pH [19], thus making Fe^{III} a much less potent oxidant at neutral pH. The E^0 fall is expected to be even larger in the presence of phosphate ions which have a higher affinity for Fe^{III} than for Fe^{II}. The same trend is observed upon iron-EDTA binding ($\log K = 25$ with Fe^{III} and 14.3 with Fe^{II}). Indeed, the experimental E^0 value for the Fe^{III}/Fe^{II} (EDTA) couple is 0.12 V. Since the redox potential of the $QH^{\cdot}/QH_2$ couple at pH 7 is 0.33 V [37], the direct electron transfer from quercetin to Fe^{III} (in the presence or absence of EDTA) can be predicted to be a thermodynamically unfavourable reversible process.

Free Radic Res Downloaded from informahealthcare.com by Library of Health Sci-Univ of Il on 11/30/11
For personal use only.

RIGHTSLINK

Under noncomplexing conditions (EDTA), iron-mediated quercetin autoxidation could be initiated either by a reversible direct electron transfer from quercetin to Fe^{III} (driven to products by the fast disproportionation of the quercetin radicals [40]) or via labile high-spin complexes, possibly monocatecholate complexes (noted $QHFe^{III}$ in Scheme 1). Both mechanisms have been reported in the literature with other catechol ligands [41,42]. In our kinetic analysis, the detection of an intermediate species absorbing at 380 nm (Tables V and VI) is more in favour of the second mechanism. Since Fe^{II} and Fe^{III} are as effective at accelerating quercetin autoxidation in the presence of EDTA, we may also assume that Fe^{II} autoxidation is not the rate-determining step of Fe^{II}-induced quercetin autoxidation. Processes likely involved in quercetin autoxidation in the presence of Fe ions are summarized in Scheme 2.

In equimolar iron ion-quercetin solutions (10^{-4} M), a low slowly increasing H_2O_2 concentration can be detected over 1 h (Figure 8) that does not exceed 10^{-5} M. Hence, it is suggested that H_2O_2 formed during quercetin autoxidation is decomposed by the Fe ions. The ROS thus produced (e.g. hydroperoxyl and hydroxyl radicals) could themselves take part in quercetin oxidation. This is in agreement with a previous work in which the hydroxyl radical could be evidenced by ESR after spin trapping in mildly alkaline solutions (pH 8.5 tris buffer, 25°C) of quercetin in the presence of Fe^{III}-EDTA [17]. The ESR signal was enhanced by superoxide dismutase and abolished by catalase, thus confirming that H_2O_2 was the precursor of the hydroxyl radical in such conditions. Hence, in the presence of iron ions, quercetin autoxidation may be a combination of the following processes (written for simplicity as overall two-electron oxidations although sequential one-electron transfers must take place):

$$QH_2(\text{and/or } QFe^{III}) + O_2 \rightarrow QS + H_2O_2$$

$$QH_2(\text{and/or } QFe^{III}) + H_2O_2 \rightarrow QS + 2H_2O$$

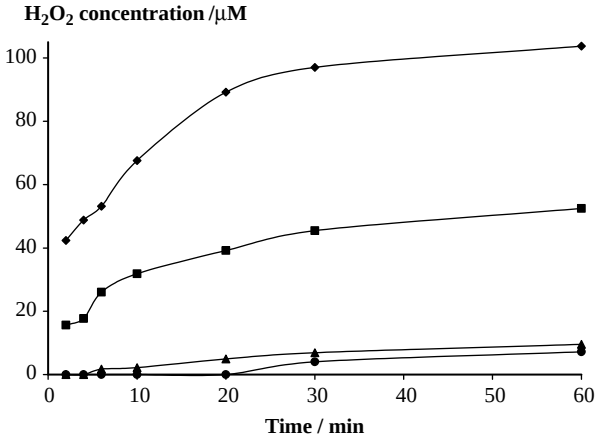

Figure 8. Production of H_2O_2 in a 0.01 M phosphate buffer (pH 7.4, 37°C) in the presence of quercetin (10^{-4} M) and metal ions (10^{-4} M): quercetin + Cu^{I} (◆), quercetin + Cu^{II} (■), quercetin + Fe^{II} (▲), quercetin + Fe^{III} (•).

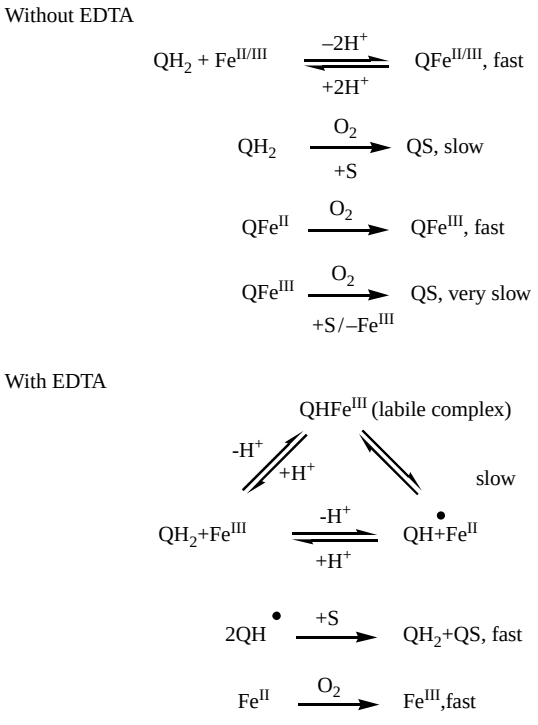

Scheme 2. Proposed mechanism for autoxidation of quercetin in the presence of iron ions (in the absence of EDTA, strong complexation is assumed to take place on the B-ring with removal of protons at O3′–H and O4′–H).

Autoxidation in presence of copper ions at pH 7.4

When the spectral changes following the addition of copper ions to a solution of quercetin in a neutral phosphate buffer are recorded over 1 h, it can be observed that the fast building-up of the absorption above 400 nm (metal complexes) is followed by a slower decay, which, however, appears much faster than with the iron ions (Figure 9). This decay (typically monitored at 460 or 420 nm for Cu^{II}/quercetin molar ratios higher than 1) is paralleled by the increase in A(330 nm) typical of the quercetin oxidation products. With Cu^{II}, no evidence could be gained that these spectral changes reflect a multi-step process. Hence, the A(460 or 420 nm) and A(330 nm) vs time curves were simultaneously fitted to a simple kinetic law assuming the first-order conversion of the metal complexes into oxidation products. The corresponding rate constants k_a lie in the range $3–9 \times 10^{-4}\ s^{-1}$ and have no clear dependence on the total Cu^{II} concentration (Table VII). As expected, the presence of EDTA (EDTA/quercetin molar ratio = 10) inhibits copper-quercetin binding (no

Free Radic Res Downloaded from informahealthcare.com by Library of Health Sci-Univ of Il on 11/30/11
For personal use only.

RIGHTSLINK

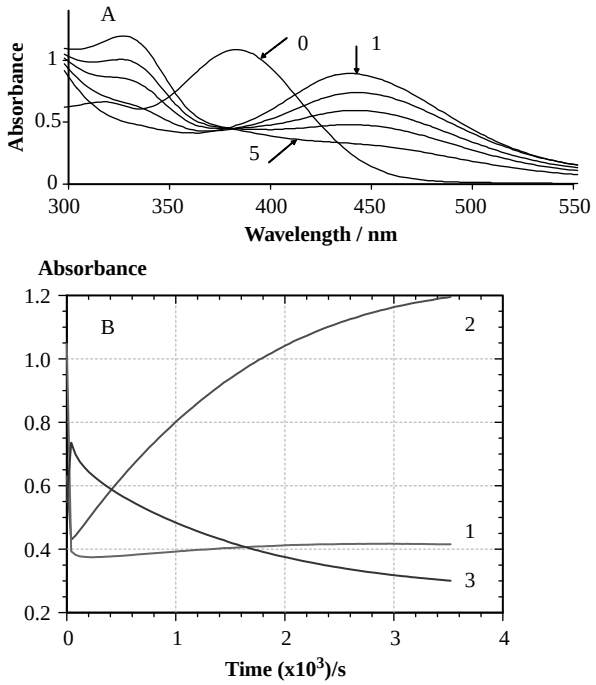

Figure 9. Autoxidation of quercetin (5×10^{-5} M) after addition of Cu^{II} (3 equiv) in a 0.01 M phosphate buffer (pH 7.4, 37°C). (Part A) UV–visible spectra at time 0 (spectrum 0), 2 min (spectrum 1), 10 min (spectrum 2), 20 min (spectrum 3), 30 min (spectrum 4) and 60 min (spectrum 5). (Part B) absorbance vs time curves. (Curve 1) detection at 380 nm. (Curve 2) detection at 330 nm. (Curve 3) detection at 420 nm.

Table VII. Autoxidation of quercetin (5×10^{-5} M) in the presence of Cu^{II} in a 0.01 M phosphate buffer (pH 7.4, 37°C). In the absence of EDTA, the spectral changes occurring during 2 min following the addition of Cu^{II} are not considered in the calculations (fast metal binding, marginal oxidation). Values in brackets are the wavelengths of detection (in nm).

Cu^{II} conc./μM	$10^5\ k_a$ s	$\varepsilon_{QS}/M^{-1}cm^{-1}$
50(330)*	27.9(± 0.4)	33210
(420)		2650
75(330)*	51.1(± 0.6)	23680
(420)		3220
100(330)*	85.5(± 0.3)	17210
(420)		3550
125(330)*	69.4(± 0.4)	22820
(420)		4500
150(330)*	60.8(± 0.5)	26170
(420)		4790
200(330)*	75.5(± 0.5)	22960
(420)		5200
50(330)†	18.8(± 0.9)	23220
(380)		7970
100(330)†	14.3(± 0.7)	25000
(380)		6500
150(330)†	21.6(± 0.9)	21660
(380)		7600
200(330)†	9.0(± 0.1)	29780
(380)	0	0

* No EDTA. † With EDTA (0.5 mM).

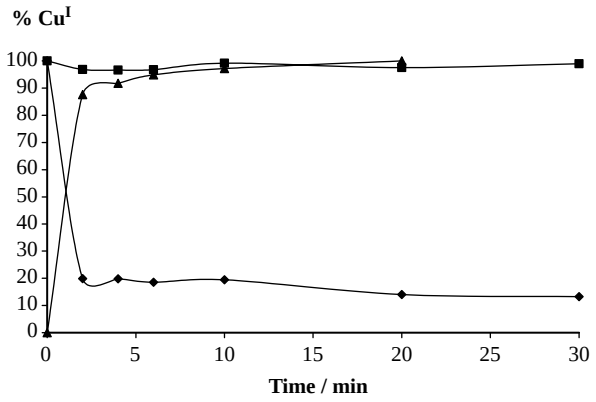

Figure 10. Time-dependence of the Cu^I concentration in a 0.01 M phosphate buffer (pH 7.4, 37°C). Copper ion and quercetin concentrations are 10^{-4} M: Cu^I (◆), Cu^I + quercetin (■), Cu^{II} + quercetin (▲).

absorption above 400 nm). The A(380 nm) and A(330 nm) vs time curves, respectively, featuring the consumption of quercetin and formation of its oxidation products were kinetically analyzed to extract the apparent first-order rate constants of autoxidation k_a. The k_a values are essentially constant and fall in the range $1–2 \times 10^{-4}\ s^{-1}$. Hence, EDTA significantly inhibits the Cu^{II}-initiated autoxidation of quercetin, which suggests that the Cu^{II}-quercetin complexes are key-autoxidation intermediates in the absence of EDTA.

In the literature, Cu^{II} has been reported to accelerate 1,2,4-benzenetriol autoxidation much more efficiently than Fe^{III} [43]. During Cu^{II}-initiated autoxidation of quercetin, H_2O_2 accumulates more readily (*ca.* 5×10^{-5} M in an equimolar 10^{-4} M mixture of quercetin and Cu^{II} after 1 h) than in the presence of the iron ions (Figure 8). Moreover, Cu^{II} is rapidly reduced into Cu^I (Figure 10) in agreement with previous reports [38].

As judged by the fast decay of A(460 nm) and building-up of A(330 nm), Cu^I-induced autoxidation of quercetin seems a quite efficient process (Figure 11). However, monitoring at 380 nm (absorption maximum of quercetin) clearly shows that the chemical transformations that follow the fast Cu^I-quercetin binding (completed in less than 20 s) are actually multi-step. The A(380 nm) vs time curves could be fitted assuming the successive conversion of the metal complex into three new species (P_1, P_2 and P_3) with apparent first-order rate constants k'_1, k'_2 and k'_3. Then, the simultaneous fitting of the A(460 nm) and A(330 nm) vs time curves with k'_1 held to its value deduced from the kinetic analysis at 380 nm yields refined values for the rate constant k'_2. Rate constants k'_1, k'_2 and k'_3 rate constants display values in the ranges $1–2 \times 10^{-2}$, $1–3 \times 10^{-3}$ and $4–5 \times 10^{-5}\ s^{-1}$, respectively (Table VIII). As for the iron ions, product P_1,

Free Radic Res Downloaded from informahealthcare.com by Library of Health Sci-Univ of Il on 11/30/11
For personal use only.

RIGHTSLINK

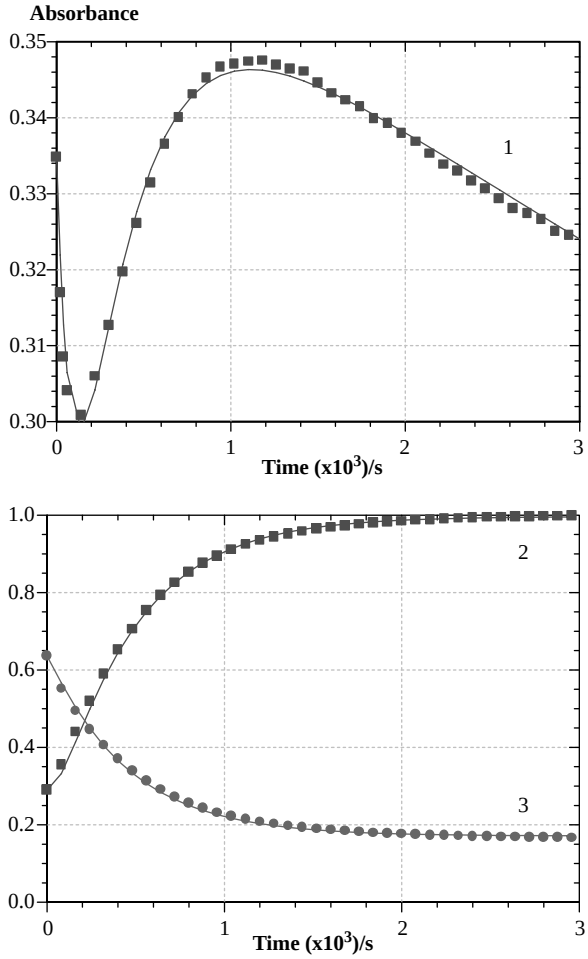

Figure 11. Autoxidation of quercetin (5×10^{-5} M) after addition of Cu^I (2 equiv) in a 0.01 M phosphate buffer (pH 7.4, 37°C). (Curve 1) detection at 380 nm. (Curve 2) detection at 330 nm. (Curve 3) detection at 420 nm. The solid lines are the results of the curve-fitting procedures.

which moderately absorbs at 330 nm and displays a strong absorption above 400 nm, must be a Cu^I-quercetin complex resulting from a rearrangement of the primary complex formed within 10–20 s after Cu^I addition (Figure 4, Table IV). During this step, no large increase in A(330 nm) can be observed so that the molar absorption coefficient at 330 nm of the new species formed is set equal to that of quercetin for the curve-fittings (experiments over 1 h). It can be noticed that a similar two-step process operates in the Cu^{II}-quercetin binding. However, because the subsequent autoxidation of quercetin is slower in that case, the time zero of the kinetic analysis of autoxidation can be delayed so as to essentially deal with the second step (rate constant k'_2). Since A(330 nm) sharply increases during the step characterized by rate constant k'_2, we assume that this parameter can be equated to the apparent rate constant of Cu^I-initiated quercetin autoxidation (k_a). This is in agreement with product P_2 having a strong absorption at 330 nm and only a very weak absorption above 400 nm. Hence, P_2 is identified as QS, the mixture of solvent adducts on the quercetin *p*-quinonemethide displaying either a five- or six-membered heterocycle (Scheme 1). Those species in equilibrium probably bind Cu^I through their catechol and/or keto groups and become further autoxidized into product P_3 (rate constant k'_3).

In the pH 7.4 phosphate buffer at 37°C, kinetics of Cu^I autoxidation are too fast to be investigated by sample uptake for spectroscopic measurements (Figure 10). Simultaneously, a rather low production of H_2O_2 can be detected that tends to level off after 15 min (data not shown). Interestingly, quercetin (in equimolar 10^{-4} M concentration with Cu^I) stimulates H_2O_2 production, allowing the formation of a quasi-stoichiometric concentration of H_2O_2 after 1 h (Figure 8). Moreover, in the presence of quercetin, Cu^I autoxidation is totally prevented (Figure 10). Since Cu^I is stabilized despite quercetin consumption, it can be concluded that the quercetin oxidation products themselves bind Cu^I (in agreement with the kinetic analysis above) and inhibit its autoxidation.

Table VIII. Autoxidation of quercetin (5×10^{-5} M) in the presence of Cu^I in a 0.01 M phosphate buffer (pH 7.4, 37°C). The spectral changes occurring during 40 s following the addition of Cu^I are not considered in the calculations (fast metal binding, marginal oxidation). Values in brackets are the wavelengths of detection (in nm).

Cu^I conc./μM	10^4 k'_1 s	10^5 k'_2 s	10^5 k'_3 s	ε'_i/$M^{-1}cm^{-1}$
50(380)*	174(±5)	–	–	5780
50(330)	174	75(±2)	4.0(±0.1)	24090, 0†
(460)				9200, 420, 0
100(380)	118(±5)	284(±8)	4.3(±0.1)	5410, 7240, 0
100(330)	118	226(±1)	–	19930†
(460)				10110, 2320
125(380)	111(±5)	318(±11)	4.6(±0.1)	5190, 7240, 0
125(330)	111	242(±1)	–	19840†
(460)				10270, 2410
150(380)	96(±5)	390(±18)	4.4(±0.1)	5370, 7540, 0
150(330)	96	261(±1)	–	20280, 0†
(460)				10370, 2610, 0

* Analysis of the fast step only. † At 330 nm, ε'_1 set equal to ε_{QH_2}.

Free Radic Res Downloaded from informahealthcare.com by Library of Health Sci-Univ of Il on 11/30/11
For personal use only.

RIGHTSLINK

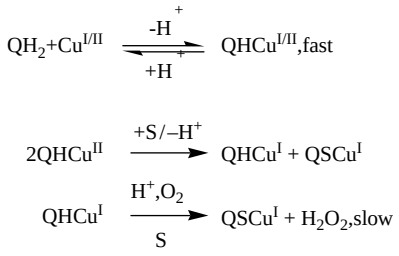

Scheme 3. Proposed mechanism for copper-induced autoxidation of quercetin (binding is assumed to take place on the C-ring with removal of proton at O3–H or O5–H).

Although, a weaker oxidant than Fe^{III} in acidic conditions ($E^0(Cu^{2+}/Cu^{+}) = 0.34$ V), Cu^{II} is no less oxidizing than Fe^{III} at neutral pH because of its weaker hydrolytic properties ($E^0(Cu^{II}/Cu^{I}) = 0.15$ V) [19]. In addition, copper ions form square planar (Cu^{II}) or tetrahedral (Cu^{I}) complexes whereas iron ions prefer (distorted) octahedral geometries. Interestingly, the Cu^{II}-initiated autoxidation of 1,2,4-benzenetriol is insensitive to superoxide dismutase whereas autoxidation with no metal added or after addition of Fe^{III} is [43]. This observation led the authors to suggest that free $O_2^{\cdot-}$ is not involved in the Cu^{II}-initiated autoxidation of 1,2,4-benzenetriol which would take place via a two-electron process within a redox active Cu^{II} complex. Moreover, a detailed investigation of the oxidation of catechol by Cu^{II} has shown that the rate-limiting step is actually an intramolecular electron transfer within the catecholate-Cu^{II} complex [44]. Since the stable redox state of copper during quercetin autoxidation is actually Cu^{I} (Figure 10), the copper-induced quercetin autoxidation is proposed to take place from the quercetin-Cu^{I} complex after eventual reduction of Cu^{II} within its complex with quercetin (Scheme 3). Since H_2O_2 is accumulated during copper-initiated autoxidation of quercetin (Figure 8), it may be proposed that the complexes involving Cu^{I} and the quercetin oxidation products are not able to decompose H_2O_2 (Fenton reaction).

The rate constants for metal-quercetin complexation and quercetin autoxidation are summarized in Table IX for all metal ions investigated in this work. It must be emphasized that the whole kinetic analysis is mainly aimed at dissociating binding from autoxidation processes to give an estimation of the apparent rate constants of quercetin autoxidation (k_a). Most probably, multiple redox processes simultaneously operate in quercetin autoxidation: autoxidation of Fe^{II}, reduction of Cu^{II} by quercetin (up to 9 equiv of Cu^{II} after incubation for 2 h in a pH 7.4 phosphate buffer at 37°C [38]), Fenton reaction (at least in the presence of the Fe ions)... However, because of the distinct spectral properties of quercetin, its metal complexes and primary oxidation products, an approximate separation between metal-quercetin binding and quercetin autoxidation is possible. As judged from the k_a values (Table IX), the rate of quercetin autoxidation in the presence or absence of added metal ions varies as follows in neutral complexing conditions (no EDTA): $Cu^{I} > Cu^{II} \gg$ no metal added $> Fe^{II} \approx Fe^{III}$. The iron complexes are only weakly redox active, probably because of their low spin. The absence of discrimation between Fe^{II} and Fe^{III} is in agreement with the fast autoxidation of Fe^{II} to Fe^{III} which is not inhibited by quercetin (Figure 3). By contrast, the copper complexes are strongly redox active. Since the Cu^{I}-induced autoxidation of quercetin appears significantly faster than the Cu^{II}-induced process, it can be proposed that the reduction of Cu^{II} by quercetin (although relatively fast, see Figure 10) is rate-limiting.

Oxidation by Fe^{III} in strongly acidic conditions

When quercetin is mixed with Fe^{III} in 0.1 M HCl–MeOH (1:1), oxidation readily proceeds even under N_2 (Figure 12). By contrast, no reaction takes place with Fe^{II}. Thus, in strongly acidic conditions where Fe^{III} is essentially under its free highly oxidizing Fe^{3+} form and quercetin under its neutral unbound form, electron transfer can take place between the two species. Reduction of highly coloured Fe^{III} complexes in mildly acidic aqueous solutions is at the basis of common antioxidant tests [45]. By analogy to a kinetic model already developed for H-atom

Table IX. Rate constants for complexation and autoxidation of quercetin (5×10^{-5} M) in a 0.01 M phosphate buffer (pH 7.4, 37°C).

	$10^{-2}k_1/M^{-1}s^{-1}$*	$10^{-2}k_2/M^{-1}s^{-1}$†	$10^4\ k'_1\ s$‡	$10^5\ k_a\ s$¶
No metal added	–	–	–	6
Fe^{III}	20–40	0.5–2	4–18	2–4
Fe^{II}	70–120	10–20	3–17	2–4
Fe^{III}–EDTA	–	–	–	20–30
Fe^{II}–EDTA	–	–	–	20–30
Cu^{II}	40–80	–	300–400	30–90
Cu^{I}	130–170	–	100–200	100–400§
Cu^{II}–EDTA	–	–	–	10–20

* 1:1 metal-quercetin binding. † 2:1 metal-quercetin binding. ‡ Slow rearrangement in the coordination sphere. ¶ Autoxidation with formation of QS. § Slow autoxidation of QS ($k_{a2} = 4–5 \times 10^{-5}\ s^{-1}$.

Free Radic Res Downloaded from informahealthcare.com by Library of Health Sci-Univ of Il on 11/30/11
For personal use only.

RIGHTSLINK

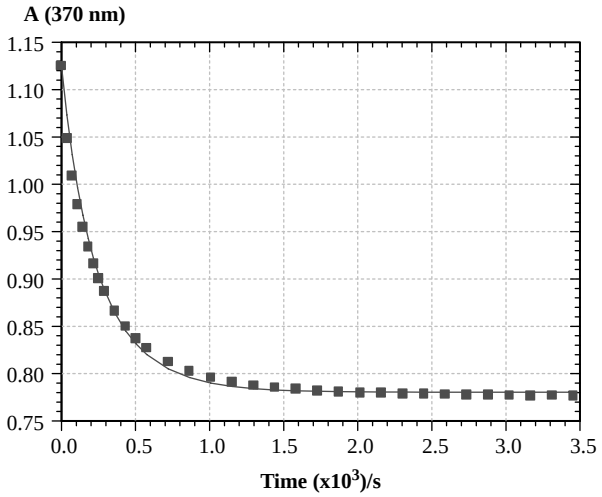

Figure 12. Oxidation of quercetin (5×10^{-5} M) by Fe^{3+}(2.5 equiv) in 0.1 M HCl–MeOH (1:1) (37°C). The solid line is the result of the curve-fitting procedure (see text).

transfer reactions from polyphenols to the DPPH radical [46], the decay of the visible absorbance of quercetin at 370 nm can be analyzed to evaluate the stoichiometry n of the reaction (number of Fe^{3+} ions reduced per quercetin molecule over 1 h of reaction) and the rate constant k_1 for the first electron transfer from quercetin. To that purpose, it is simply assumed that quercetin is made of n reducing units R that all irreversibly transfer one electron to Fe^{3+} with the same bimolecular rate constant k: $R + Fe^{3+} \rightarrow R_{ox} + Fe^{2+}$. For the Fe^{III}/quercetin molar ratios selected (in the range 1–5), a fraction of quercetin is spared at the end of the reaction as evidenced by the residual absorbance at 370 nm (Figure 12). Once this plateau is reached, it is assumed that all Fe^{3+} has been converted into Fe^{2+}.

The following equations can thus be used in the curve-fitting procedure:

$$A = \varepsilon[QH_2] = \varepsilon[R]/n$$

$$-\frac{d}{dt}[R] = -\frac{d}{dt}[Fe^{3+}] = k[R][Fe^{3+}]$$

The initial concentrations are $(R)_0 = nA_0/\varepsilon$, $(Fe^{3+})_0 = C$. The initial rate of quercetin consumption can also be written as: $k(R)_0(Fe^{3+})_0 = kn(QH_2)_0(Fe^{3+})_0 = k_1(QH_2)_0(Fe^{3+})_0$. Hence, k can be identified with k_1/n. The values for k_1 and n are collected in Table X. As a validation of the simplified data treatment exposed above, these values are in reasonable agreement for the different Fe^{3+} concentrations used. From the n values, it is clear that quercetin undergoes an extensive oxidative degradation in those conditions since a single quercetin molecule is able to reduce *ca.* seven Fe^{3+} ions after 1 h of reaction. This value is only a lower limit since A(370 nm) continues to slightly decay beyond 1 h.

Table X. Reduction of Fe^{III} by quercetin (5×10^{-5} M) in 0.1 M HCl–MeOH (1:1) (37°C) Molar absorption coefficient of quercetin at 370 nm = 2×10^4 $M^{-1}cm^{-1}$.

Fe^{III}/μM	$k_1/M^{-1}s^{-1}$*	n†
50	55(± 1)	7.34(± 0.02)
75	49(± 1)	7.12(± 0.04)
125	82(± 1)	7.26(± 0.01)
250	89.0(± 0.3)	6.67(± 0.01)

*Rate constant for the first electron transfer from quercetin. †Stoichiometry (number of Fe^{III} reduced per molecule of quercetin over 1 h).

Such high n values are in agreement with those measured in DPPH scavenging experiments [46] ($n \approx 5$) and in the reduction of Cu^{II} by quercetin ($n \approx 9$) [38].

Conclusion

Quercetin, one of the most abundant flavonoids in plants and food, displays contrasted behaviours with iron and copper ions. In strongly acidic conditions where Fe^{III} is a potent oxidant, quercetin rapidly reduces up to 7 equiv of Fe^{3+} without participation of dioxygen. In mildly acidic conditions (pH 5), quercetin quickly binds iron ions with no simultaneous autoxidation. In neutral conditions, quercetin even more quickly binds iron and copper ions (although competition with the phosphate ions from the buffer is very significant). Following complexation, quercetin is oxidized by dioxygen (autoxidation) via distinct mechanisms. In the case of iron ions, the complexes are relatively inert and react with dioxygen even more slowly than free quercetin. Addition of EDTA inhibits iron-quercetin binding and promotes quercetin autoxidation. In the case of the copper ions, the thermodynamically stable complexes are rapidly autoxidized, the reduction of Cu^{II} by quercetin being the likely rate-determining step. Addition of EDTA inhibits copper-quercetin binding and quercetin autoxidation. Those processes may be of importance in the field of food chemistry since polyphenols and metal ions may come into contact during food processing, conservation and cooking and also in the field of nutrition. Indeed, after food ingestion, significant concentrations of labile iron and copper complexes can be produced in the gastro-intestinal tract because of the catabolism of endogenous ligands [47,48]. Their role in accelerating the autoxidation of dietary antioxidants, thereby altering their bioavailability, certainly deserves more attention.

Acknowledgements

The authors wish to thank the comité mixte inter-universitaire franco-marocain (CMIFM) for financial support (PAI MA/03/85).

Free Radic Res Downloaded from informahealthcare.com by Library of Health Sci-Univ of Il on 11/30/11
For personal use only.

RIGHTSLINK

Free Radic Res Downloaded from informahealthcare.com by Library of Health Sci-Univ of Il on 11/30/11
For personal use only.

References

[1] Harborne JB, Williams CA. Advances in flavonoid research since 1992. Phytochemistry 2000;55:481–504.

[2] Havsteen BH. The biochemistry and medical significance of flavonoids. Pharmacol Ther 2002;96:67–202.

[3] Parr AJ, Bolwell GP. Phenols in the plant and in man. The potential for possible nutritional enhancement of the diet by modifying the phenol content and profile. J Sci Food Agric 2000;80:985–1012.

[4] Haslam E. Natural polyphenols (vegetable tannins) as drugs: Possible modes of action. J Nat Prod 1996;59:205–215.

[5] Pietta PG. Flavonoids as antioxidants. J Nat Prod 2000;63: 1035–1042.

[6] Moran JF, Klucas RV, Grayer RJ, Abian J, Becana M. Complexes of iron with phenolic compounds from soybean nodules and other legume tissues: Prooxidant and antioxidant properties. Free Radic Biol Med 1997;22:861–870.

[7] Hurrell RF, Reddy M, Cook JD. Inhibition of non-haem iron absorption in man by polyphenolic-containing beverages. Br J Nutr 1999;81:289–295.

[8] Puppo A. Effect of flavonoids on hydroxyl radical formation by Fenton-type reactions; influence of the iron chelator. Phytochemistry 1992;31:85–88.

[9] Laughton MJ, Halliwell B, Evans PJ, Hoult JRS. Antioxidant and pro-oxidant actions of the plant phenolics quercetin, gossypol and myricetin. Effect on lipid peroxidation, hydroxyl radical generation and bleomycin-dependent damage to DNA. Biochem Pharmacol 1989;38:2859–2865.

[10] Hanasaki Y, Ogawa S, Fukui S. The correlation between active oxygens scavenging and antioxidative effects of flavonoids. Free Radic Biol Med 1994;16:845–850.

[11] Yoshino M, Murakami K. Interaction of iron with polyphenolic compounds: Application to antioxidant characterization. Anal Biochem 1998;257:40–44.

[12] van Acker SABE, van Balen GP, van den Berg DJ, Bast A, van der Vijgh WJF. Influence of iron chelation on the antioxidant activity of flavonoids. Biochem Pharmacol 1998;56:935–943.

[13] Sugihara N, Arakawa T, Ohnishi M, Furuno K. Anti- and pro-oxidative effects of flavonoids on metal-induced lipid hydroperoxide-dependent lipid peroxidation in cultured hepatocytes loaded with α-linolenic acid. Free Radic Biol Med 1999;27:1313–1323.

[14] Cao G, Sofic E, Prior RL. Antioxidant and prooxidant behaviour of flavonoids:structure–activity relationships. Free Radic Biol Med 1997;22:749–760.

[15] Sestili P, Guidarelli A, Dacha M, Cantoni O. Quercetin prevents DNA single strand breakage and cytotoxicity caused by tert-butylhydroperoxide: Free radical scavenging versus iron chelating mechanism. Free Radic Biol Med 1998; 25:196–200.

[16] Yamashita N, Tanemura H, Kawanishi S. Mechanism of oxidative DNA damage induced by quercetin in the presence of Cu(II). Mutat Res 1999;425:107–115.

[17] Canada AT, Giannella E, Nguyen TD, Mason RP. The production of reactive oxygen species by dietary flavonols. Free Radic Biol Med 1990;9:441–449.

[18] Long LH, Clement MV, Halliwell B. Artifacts in cell culture: Rapid generation of hydrogen peroxide on addition of (−)-epigallocatechin, (−)-epigallocatechin gallate, (+)-catechin and quercetin to commonly used cell culture media. Biochem Biophys Res Commun 2000;273:50–53.

[19] Miller DM, Buettner GR, Aust SD. Transition metals as catalysts of autoxidation reactions. Free Radic Biol Med 1990;8:95–108.

[20] Wee LM, Long LH, Whiteman M, Halliwell B. Factors affecting the ascorbate- and phenolic-dependent generation of hydrogen peroxide in Dulbecco's modified Eagles medium. Free Radic Res 2003;37:1123–1130.

[21] Galati G, Moridani MY, Chan TS, O'Brien PJ. Peroxidative metabolism of apigenin and naringenin versus luteolin and quercetin: Glutathione oxidation and conjugation. Free Radic Biol Med 2001;30:370–382.

[22] Galati G, Sabzevari O, Wilson JX, O'Brien PJ. Prooxidant activity and cellular effects of the phenoxyl radicals of dietary flavonoids and other polyphenolics. Toxicology 2002;177: 91–104.

[23] Galati G, O'Brien PJ. Flavonois and isoflavones (phytoestrogens): Absorption, metabolism, and bioactivity. Free Radic Biol Med 2004;37:287–303.

[24] Boersma MG, Vervoort J, Szymusiak H, Lemanska K, Tyrakowska B, Cenas N, Segura-Aguilar J, Rietjens IMCM. Regioselective and reversibility of the glutathione conjugation of quercetin quinone methide. Chem Res Toxicol 2000;13: 185–191.

[25] Awad HM, Boersma MG, Boeren S, van Bladeren PJ, Vervoort J, Rietjens IMCM. Structure-activity study of the quinone/quinone methide chemistry of flavonoids. Chem Res Toxicol 2001;14:398–408.

[26] Metodiewa D, Jaiswal AK, Cenas N, Dickancaite E, Segura-Aguilar J. Quercetin may act as a cytotoxic prooxidant after its metabolic activation to semiquinone and quinonoidal product. Free Radic Biol Med 1999;26:107–116.

[27] Makris DP, Rossiter JT. Heat-induced, metal-catalyzed oxidative degradation of quercetin and rutin (quercetin 3-*O*-rhamnosylglucoside) in aqueous model systems. J Agric Food Chem 2000;48:3830–3838.

[28] Sodergren E, Nourooz-Zadeh J, Berglund L, Vessby B. Re-evaluation of the ferrous oxidation in xylenol orange assay for the measurement of plasma lipid hydroperoxides. J Biochem Biophys Methods 1998;37:137–146.

[29] Welch KD, Davis TZ, Aust SD. Iron autoxidation and free radical generation: Effects of buffers, ligands, and chelators. Arch Biochem Biophys 2002;397:360–369.

[30] Midorikawa K, Uchida T, Okamoto Y, Toda C, Sakai Y, Ueda K, Hiraku Y, Murata M, Kawanishi S, Kojima N. Metabolic activation of carcinogenic ethylbenzene leads to oxidative DNA damage. Chem Biol Int 2004;150:271–281.

[31] Jungbluth G, Ruhling I, Ternes W. Oxidation of flavonols with Cu(II), Fe(II) and Fe(III) in aqueous medium. J Chem Soc Perkin Trans 2 2000;1946–1952.

[32] Utaka M, Takeda A. Copper(II)-catalysed oxidation of quercetin and 3-hydroxyflavone. J Chem Soc Chem Commun 1985;1824–1826.

[33] Dangles O, Fargeix G, Dufour C. One-electron oxidation of quercetin and quercetin derivatives in protic and non protic media. J Chem Soc Perkin Trans 2 1999;1387–1395.

[34] Jorgensen LV, Cornett C, Justesen U, Skibsted LH, Dragsted LO. Two-electron electrochemical oxidation of quercetin and kaempferol changes only the flavonoid C-ring. Free Radic Res 1998;29:339–350.

[35] Krishnamachari V, Levine LH, Pare PW. Flavonoid oxidation by the radical generator AIBN: A unified mechanism for quercetin radical scavenging. J Agric Food Chem 2002;50: 4357–4363.

[36] Escandar GM, Sala LF. Complexing behavior of rutin and quercetin. Can J Chem 1991;69:1994–2001.

[37] Jovanovic SV, Steenken S, Hara Y, Simic MG. Reduction potentials of flavonoid and model phenoxyl radicals. Which ring in flavonoids is responsible for the antioxidant activity? J Chem Soc Perkin Trans 2 1996;2497–2504.

[38] Mira L, Fernandez MT, Santos M, Rocha R, Florencio MH, Jennings KR. Interactions of flavonoids with iron and copper ions: A mechanism for their antioxidant activity. Free Radic Res 2002;36:1199–1208.

[39] Engelmann MD, Hutcheson R, Cheng IF. Stability of ferric complexes with 3-hydroxyflavone (flavonol), 5,7-dihydroxy-

RIGHTSLINK

flavone (chrysin), and 3′,4′-dihydroxyflavone. J Agric Food Chem 2005;53:2953–2960.

[40] Bors W, Michel C, Schikora S. Interaction of flavonoids with ascorbate and determination of their univalent redox potentials: A pulse radiolysis study. Free Radic Biol Med 1995;19:45–52.

[41] Hynes MJ, Coinceanainn MO. The kinetics and mechanisms of the reaction of iron(III) with gallic acid, gallic acid methyl ester and catechin. J Inorg Chem 2001;85:131–142.

[42] Jameson GNL, Linert W. The oxidation of 6-hydroxydopamine in aqueous solution. Part 3. Kinetics and mechanism of the oxidation with iron(III). J Chem Soc Perkin Trans 2 2001;569–575.

[43] Zhang L, Bandy B, Davison AJ. Effects of metals, ligands and antioxidants on the reaction of oxygen with 1,2,4-benzenetriol. Free Radic Biol Med 1996;20:495–505.

[44] Kamau P, Jordan RB. Kinetic study of the oxidation of catechol by aqueous copper(II). Inorg Chem 2002;41: 3076–3083.

[45] Pulido R, Bravo L, Saura-Calixto F. Antioxidant activity of dietary polyphenols as determined by a modified ferric reducing/antioxidant power assay. J Agric Food Chem 2000;48:3396–3402.

[46] Goupy P, Dufour C, Loonis M, Dangles O. Quantitative kinetic analysis of hydrogen transfer reactions from dietary polyphenols to the DPPH radical. J Agric Food Chem 2003;51:615–622.

[47] Halliwell B, Zhao K, Whiteman M. The gastrointestinal tract: A major site of antioxidant action? Free Radic Res 2000;33: 819–830.

[48] Halliwell B, Rafter J, Jenner A. Health promotion by flavonoids, tocopherols, tocotrienols, and other phenols: Direct or indirect effects? Antioxidant or not? Am J Clin Nutr 2005;81:268S–276S.

Free Radic Res Downloaded from informahealthcare.com by Library of Health Sci-Univ of Il on 11/30/11
For personal use only.

RIGHTSLINK